Discovery of a Potent Inhibitor of the Antiapoptotic Protein Bcl-x_L from NMR and Parallel Synthesis

Andrew M. Petros,† Jurgen Dinges,† David J. Augeri, Steven A. Baumeister, David A. Betebenner, Mark G. Bures, Steven W. Elmore, Philip J. Hajduk, Mary K. Joseph, Shelley K. Landis, David G. Nettesheim, Saul H. Rosenberg, Wang Shen, Sheela Thomas, Xilu Wang, Irini Zanze, Haichao Zhang, and Stephen W. Fesik*

Global Pharmaceutical Research and Development, Abbott Laboratories, Abbott Park, Illinois 60064

Received August 1, 2005

The antiapoptotic proteins Bcl-x_L and Bcl-2 play key roles in the maintenance of normal cellular homeostasis. However, their overexpression can lead to oncogenic transformation and is responsible for drug resistance in certain types of cancer. This makes Bcl-x_L and Bcl-2 attractive targets for the development of potential anticancer agents. Here we describe the structure-based discovery of a potent Bcl-x_L inhibitor directed at a hydrophobic groove on the surface of the protein. This groove represents the binding site for BH3 peptides from proapoptotic Bcl-2 family members such as Bak and Bad. Application of NMR-based screening yielded an initial biaryl acid with an affinity (K_d) of ~300 μM for the protein. Following the classical "SAR by NMR" approach, a second-site ligand was identified that bound proximal to the first-site ligand in the hydrophobic groove. From NMR-based structural studies and parallel synthesis, a potent ligand was obtained, which binds to Bcl-x_L with an inhibition constant (K_i) of 36 ± 2 nM.

Introduction

Apoptosis (programmed cell death) plays a vital role in normal development, tissue remodeling, immune response, and overall maintenance for all multicellular organisms.[1,2] Disruption of this process is implicated in a number of disease states, including Alzheimers disease, autoimmune disorders, and cancer. The B-cell lymphoma (Bcl) family of proteins, which includes both antiapoptotic members, such as Bcl-2, Bcl-x_L, and Bcl-w, and proapoptotic members, such as Bak, Bax, and Bad, play key roles in both normal and abnormal apoptotic processes.[3] In general, homeostasis is maintained by the highly regulated expression of these pro- and antiapoptotic proteins coupled with their tissue-specific patterns of distribution. Under normal circumstances, apoptotic stimuli such as DNA damage or hypoxia induce expression and/or activation of proapoptotic family members and subsequent apoptosis of the aberrant cell. For some cancers, however, this apoptotic process is circumvented by overexpression of the antiapoptotic proteins Bcl-2 and/or Bcl-x_L.[4,5] Therefore, Bcl-2 and Bcl-x_L are attractive targets for the development of anticancer agents.[6]

The three-dimensional structures of several Bcl-2 family proteins have been determined and all display the same overall fold.[7] This fold consists of two predominately hydrophobic, central α-helices surrounded by five to seven amphipathic helices of varying length. The antiapoptotic proteins Bcl-x_L and Bcl-2 have a hydrophobic groove on their surface, which serves as the binding site for the proapoptotic proteins such as Bak, Bax, and Bad. The three-dimensional-structure of BH3 peptides from Bak and Bad bound to Bcl-x_L have been determined by NMR.[8,9] In both cases, the peptide binds as an amphipathic helix and makes key hydrophobic interactions in the groove of the protein.

A challenging aspect of targeting Bcl-x_L is that its activity is manifested through interactions with other proteins. Historically, such interactions have been difficult to disrupt using small molecules, resulting in a strong bias against targeting protein−protein interactions.[10] A primary hurdle in designing inhibitors of protein−protein interactions is that these interactions typically involve extensive surface contact between the two partners, typically 750−1500 Å^2 for each side of the interface. Protein−protein binding sites also tend to be shallow and featureless compared to small molecule binding sites. The binding site in Bcl-2 and Bcl-x_L is very different from the typical case. For Bak peptide binding to Bcl-x_L, only approximately 500 Å^2 of the protein surface is involved. Furthermore, the binding site on Bcl-x_L is a deep, hydrophobic groove. This groove accommodates an amphipathic helix upon binding of Bcl-x_L to its proapoptotic partners. Here we describe the use of fragment-based methods, specifically "SAR by NMR", and parallel synthesis to obtain a potent inhibitor that binds in the hydrophobic groove of Bcl-x_L.

Results and Discussion

Discovery of a First-Site Ligand. An NMR-based screen was conducted using a form of Bcl-x_L that lacked the putative transmembrane helix and the long unstructured loop connecting helix 1 to helix 2.[8] A 10 000 compound fragment library with an average compound molecular weight of 210 Da was screened and yielded the fluoro biaryl acid **1** (Table 1) as a ligand for Bcl-x_L. Figure 1 shows a section from a ^{15}N HSQC spectrum of Bcl-x_L in the presence (red) and absence (black) of compound **1**. The chemical shift changes (e.g., G94 and G138) observed in this region of the spectrum along with those observed in other regions are consistent with the compound binding in the hydrophobic groove of Bcl-x_L. An NMR-based titration of this compound yielded a dissociation constant (K_d) of ~300 μM.

To explore the structure−activity relationships for binding to this site, several biaryl analogues from our corporate compound repository were tested for binding to Bcl-x_L. Some of these are shown in Table 1. From these studies it was clear that the carboxylate was critical for binding, as analogues containing a phenol (**3**) or methyl ester (**4**) exhibited weaker affinities compared to the corresponding acids. In addition, the position of the carboxylate proved to be important, as a shift of the acid moiety from para to meta decreased affinity (compare **5** with **2**), as did homologation of the carboxylate (compounds **6** and **7**). The fluorine atom could be replaced with either a

* To whom correspondence should be addressed. Tel: (847) 937-1201. Fax: (847) 938-2478. E-mail: stephen.fesik@abbott.com.
† These authors contributed equally to this work.

10.1021/jm0507532 CCC: $33.50
Published on Web 12/20/2005

Table 1. Affinities of Selected Biaryl Compounds for Bcl-x_L

No.	Structure	NMR K_d (μM)
1	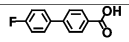	300 ± 30
2	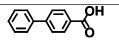	1200 ± 530
3	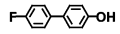	> 5000
4	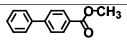	> 5000
5	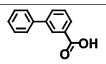	> 5000
6	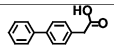	2000 ± 1600
7	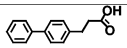	1990 ± 990
8	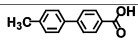	383 ± 117
9	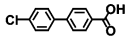	238 ± 110
10	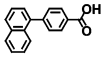	250 ± 139

Table 2. Affinities of Selected Second-Site Bcl-x_L Binders

No.	Structure	NMR K_d (μM)
11		4300 ± 1600
12		13000 ± 7000
13		5000 ± 2000
14		2000 ± 440
15		11000 ± 4800
16		13000 ± 4500
17		9000 ± 2000
18		4000 ± 2050
19		6000 ± 1970
20		6000 ±2000

methyl group (**8**) or a chlorine atom (**9**) and the fluorine-bearing ring could be replaced with a naphthalene (**10**).

NMR-based structural studies on Bcl-x_L complexed to compound **1** showed that this compound binds at the center of the hydrophobic groove[11] and occupies approximately the same position as the key leucine residue of the bound Bak peptide.[8] Furthermore, compound **1** is positioned to make an electrostatic interaction, through its carboxylate, with R139 of the protein.[11] For the Bak peptide, an analogous interaction was observed between an aspartic acid residue of the peptide (D83) and R139.

Discovery of a Second-Site Ligand. The comparison of the structure of Bcl-x_L complexed to **1** with the structure of the Bcl-x_L/Bak peptide complex indicates the existence of a proximal second site. In the structure of the Bak peptide complex, this site is filled by the side chain from I85 of the peptide. To identify ligands for this proximal site, a second-site screen was performed in the presence of an excess (2 mM) of compound **1** using a 3500 compound library with an average molecular weight of 125 Da. From this screen, several naphthol analogues and a biaryl phenol (Table 2) were identified that bound to Bcl-x_L in the presence of the fluoro biaryl acid. These second-site ligands bound to Bcl-x_L more weakly then the first-site ligands with dissociation constants in the low millimolar range. In the section of the ^{15}N HSQC spectrum shown in Figure 1, the cross-peaks from the complex of Bcl-x_L with both compounds **1** and **11** are shown in green. In addition to minor shift changes of the G94 and G138 amides, the amide of G196 shifts upon the addition of this second-site ligand. The shift changes are consistent with binding of the ligand in the hydrophobic groove of Bcl-x_L.

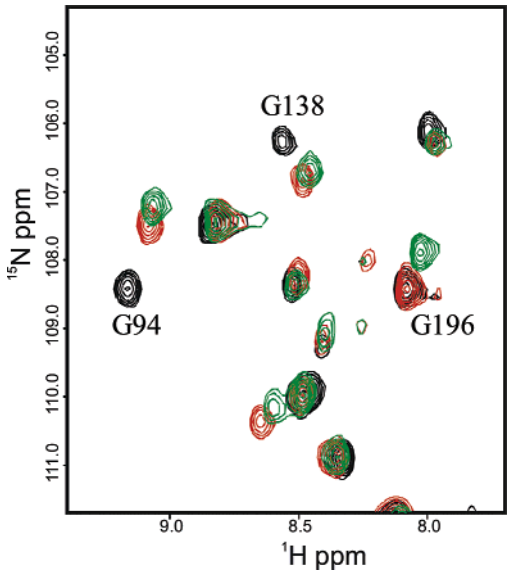

Figure 1. Selected region of ^{15}N HSQC spectra recorded on uniformly ^{15}N-labeled Bcl-x_L alone (black), in the presence of 2 mM biaryl acid **1** (red), and in the presence of 2 mM biaryl acid **1** and 5 mM naphthol derivative **11** (green).

Linking Strategy. To propose an appropriate linking strategy for these two fragments, the structure of the ternary complex of Bcl-x_L with compounds **1** and **11** was obtained using NMR.

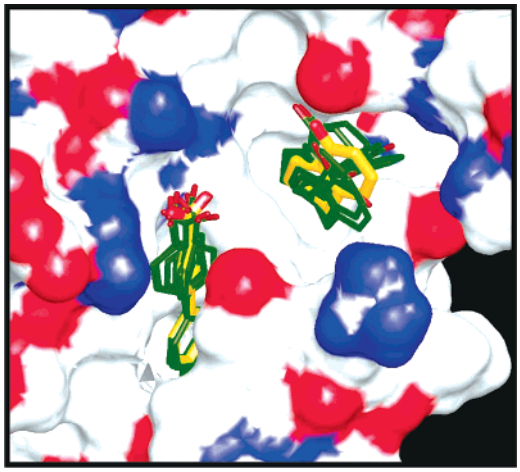

Figure 2. Superposition of seven low-energy structures calculated for Bcl-x_L complexed to **1** and **11**. For clarity, the average-minimized structure of the protein is shown as a solvent-accessible surface, color coded as follows: oxygen and oxygen-bound protons are red, and nitrogen and nitrogen-bound protons are blue, while all other atoms are gray. The positions of compounds **1** and **11** in the average-minimized structure are shown in orange.

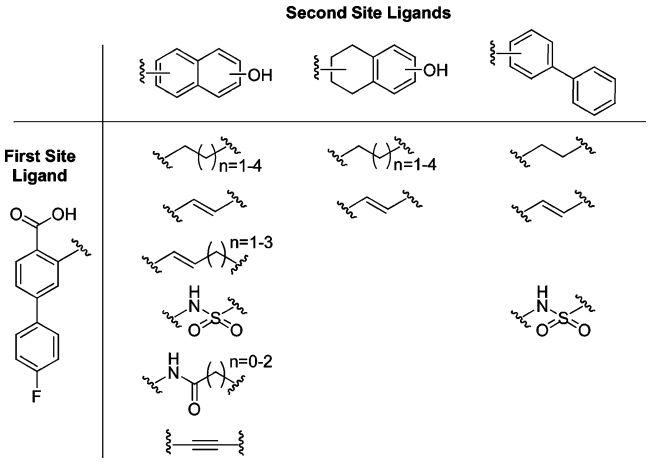

Figure 3. Fragment linking strategy used for Bcl-x_L. The best compound incorporated the second-site biaryl and a *trans*-olefin linker.

Scheme 1[a]

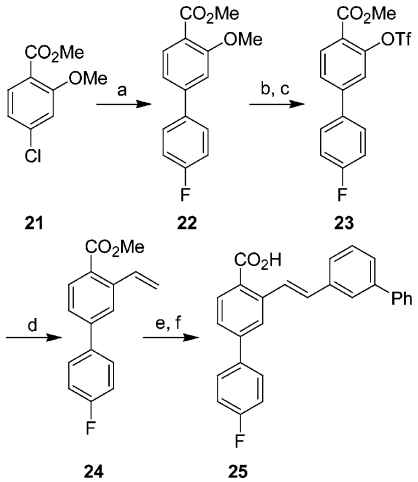

[a] Reagents and conditions: (a) 4-fluorophenylboronic acid, $PdCl_2(PCy_3)_2$, CsF, NMP; 90 °C 15 h; (b) BBr_3 DCM, −78 °C to rt, 16 h; (c) Tf_2NPh, $(i\text{-Pr})_2NEt$, DCM, 0 °C to rt; (d) vinyldibutylboronate, $Pd(PPh_3)_4$, CsF, 2:1 DME:MeOH, reflux, 15 h; (e) 3-bromobiphenyl, $Pd_2(dba)_3$, NEt_3, $P(o\text{-tol})_3$, 2:1 CH_3CN:DMF, 85 °C, 10 h; (f) LiOH·H_2O, THF, MeOH, rt, 15 h.

A superposition of seven low-energy structures for the Bcl-x_L ternary complex is shown in Figure 2. The ortho position of the biaryl acid seemed to provide the most direct trajectory to the second site. On this basis, various linkers were used to connect the ortho position of the fluoro biaryl acid to either a naphthol moiety or a biaryl moiety (Figure 3). Most of the resulting compounds bound with an inhibition constant (K_i) greater than 10 μM, as measured in a flourescence polarization assay.[12] However, compound **25** (Scheme 1), which incorporates a *trans*-olefin linker and a biaryl second-site fragment, binds to Bcl-x_L with an inhibition constant (K_i) of 1.4 ± 0.4 μM. This represents an appoximately 200-fold improvement in potency over the original biaryl acid **1**.

Structural Characterization of Linked Compound. The binding of **25** to Bcl-x_L was characterized structurally by NMR in order to uncover areas for further gains in affinity. As the solubility of this compound was limited, it was not possible to obtain NMR data of sufficient quality to do a full structure determination. However, nine unambiguous intermolecular NOEs were obtained for this ligand when bound to Bcl-x_L, from which a model was generated of the compound bound to the protein (Figure 4). The model shows that compound **25** interacts with both site 1 and site 2 in the hydrophobic groove of the protein. However, from this NMR-based model, we concluded that the

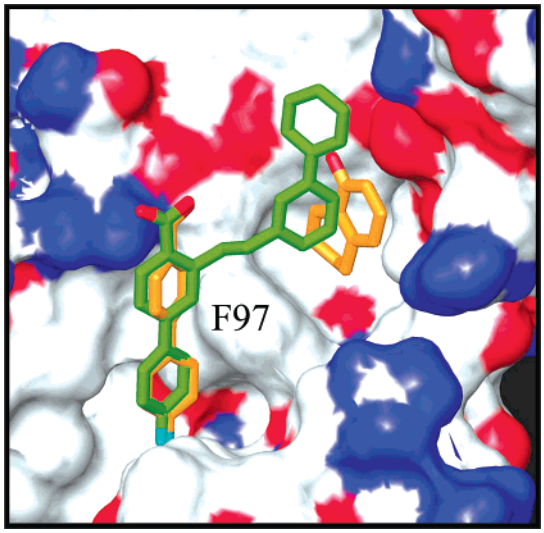

Figure 4. NMR-derived model of *trans*-olefin linked compound **25** bound to Bcl-x_L. The side chain of F97 divides the first site from the second site. Protein is shown as a solvent-accessible surface color-coded as in Figure 2.

Table 3. Affinities of Selected Acylsulfonamides for Bcl-x_L

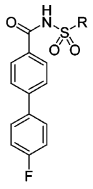

No.	R =	NMR K_d (μM)	Bcl-x_L FPA K_i (μM)
26	Me	320 ± 35	-
28	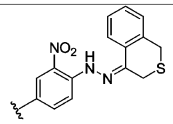	<10[a]	0.245 ± 0.013
31	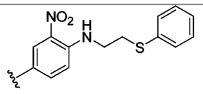	<10[a]	0.036 ± 0.002

[a] Compound in slow exchange.

trans olefin may not be the best linker for maintaining the optimal position of the first and second-site fragments and that a different trajectory from the first-site fragment might be necessary.

Discovery of Acylsulfonamide Linker. Acylsulfonamides are common isosteres for carboxylates, as they possess pK_a's in the range of 3−5. To overcome the shortcomings of the *trans*-olefin linker, it was proposed that the *p*-carboxylate of the biaryl acid be replaced with an acylsulfonamide, which could then function as a linker. The advantage of this moiety is that it can bridge the wall between the two sites while the key electrostatic interaction that the first-site ligand makes with R139 of the protein is maintained. To test whether the acylsulfonamide could serve as a suitable replacement for the carboxylic acid, methyl biaryl acylsulfonamide **26** was synthesized and tested for binding to Bcl-x_L. The methyl biaryl acylsulfonamide displayed virtually the same affinity as the biaryl acid (Table 3). On the basis of this observation, a structurally diverse set[13] of sulfonamides and sulfonyl chlorides was selected from commercial sources and our corporate compound repository to prepare a small library

Scheme 2[a]

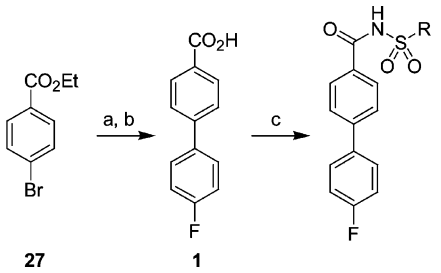

[a] Reagents and conditions: (a) $Pd(PPh_3)_4$, DME, 4-fluorophenylboronic acid in EtOH, aq Na_2CO_3, reflux, 16 h; (b) 2 N NaOH, 2:1 THF:MeOH, rt, 16 h; (c) RSO_2NH_2, P-EDC, DMAP, $ClCH_2CH_2Cl$/*t*-BuOH, rt, 24 h, then MP-TsOH, EtOAc, rt, 4 h.

of acylsulfonamides. The sulfonyl chlorides were converted to their sulfonamide analogues through reaction with ammonium hydroxide in diethyl ether at room temperature. The biphenyl acid **1** was prepared through Suzuki coupling of ethyl 4-bromobenzoate **27** with 4-fluorophenylboronic acid and followed by ester cleavage (Scheme 2). A total of 120 acylsulfonamides were then synthesized in parallel using the method of Sturino et al.,[14] which was modified to include the use of resin-bound tosic acid scavenging reagent.[15] Of these, compound **28** (Table 3) exhibited the greatest affinity for Bcl-x_L, with an inhibition constant (K_i) of 0.245 ± 0.013 μM.

Structural Characterization of Compound 28. To guide subsequent rounds of synthesis, an NMR-based structure of **28** bound to Bcl-x_L was determined. The averaged-minimized structure is shown in Figure 5. The biaryl portion of this compound makes essentially the same contacts as the original biaryl acid, with the exception that it is tilted slightly toward the second site with respect to the free acid. The nitrophenyl sits on top of F97 and below Y194, forming a hydrophobic π-stacked arrangement. This type of interaction was not observed for either the bound Bak or Bad peptide.

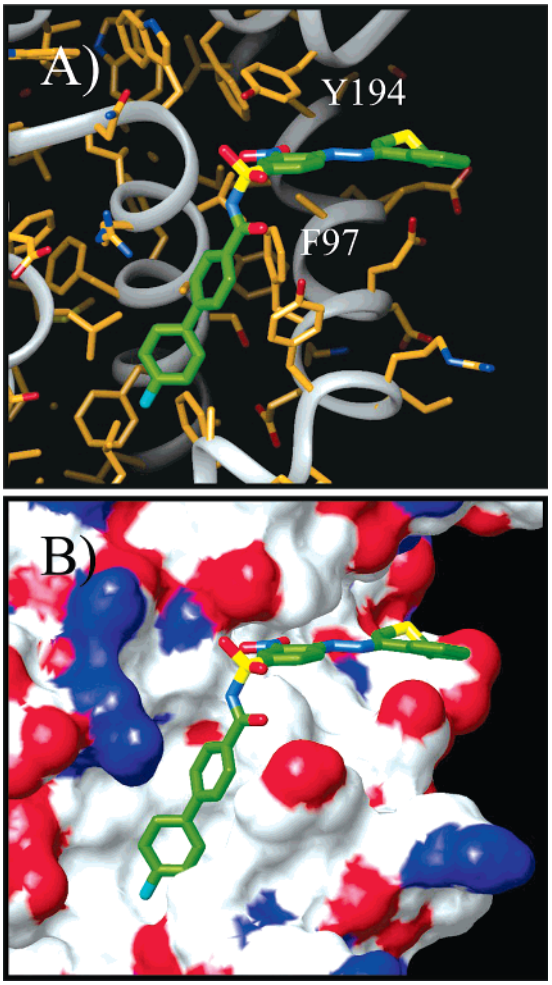

Figure 5. NMR-derived structure of acylsulfonamide compound **28** bound to Bcl-x_L. (A) The nitrophenyl portion of **28** forms a π-stack with F97 and Y194 of the protein. (B) Bcl-x_L is shown as a solvent-accessible surface. Atoms are color-coded as in Figure 2.

Scheme 3[a]

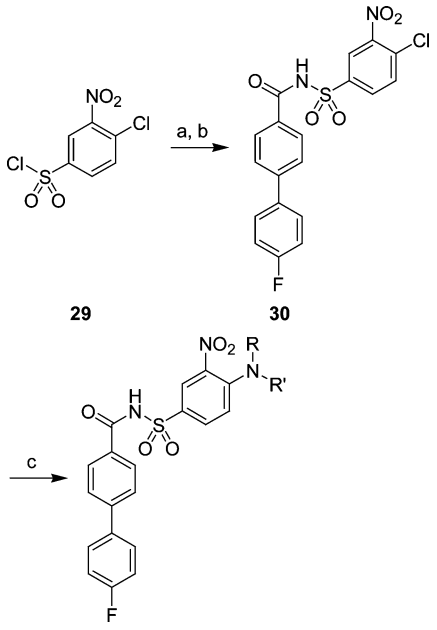

[a] Reagents and conditions: (a) NH_4OH, diethyl ether, 0 °C to rt, 30 min; (b) **1**, EDC, DMAP, CH_2Cl_2, rt, 16 h; (c) HNRR′, DMF, 100 °C, 16 h.

Second Parallel Synthesis. As the acylsulfonamide, nitrophenyl linker appeared to provide an energetically favorable way of connecting a first-site fragment to a second-site fragment, another round of parallel synthesis was carried out in order to optimize second-site binding. Toward this end, an acylsulfonamide core was prepared that contained a 4-chloro-3-nitrophenyl moiety. This core allowed the SAR to be rapidly established through the nucleophilic aromatic substitution of its 4-chloro substituent with selected amines (Scheme 3). The commercially

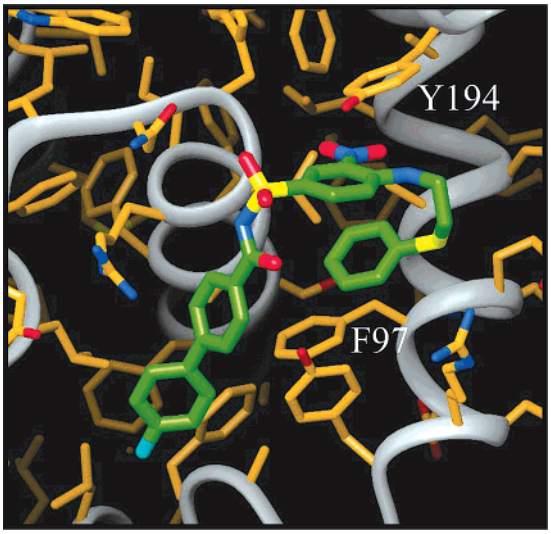

Figure 6. NMR-derived structure of compound **31** bound to Bcl-x_L. The nitrophenyl portion of **31** forms a π-stack with F97 and Y194 of the protein. In addition, the compound adopts an unexpected intramolecular π-stack arrangement.

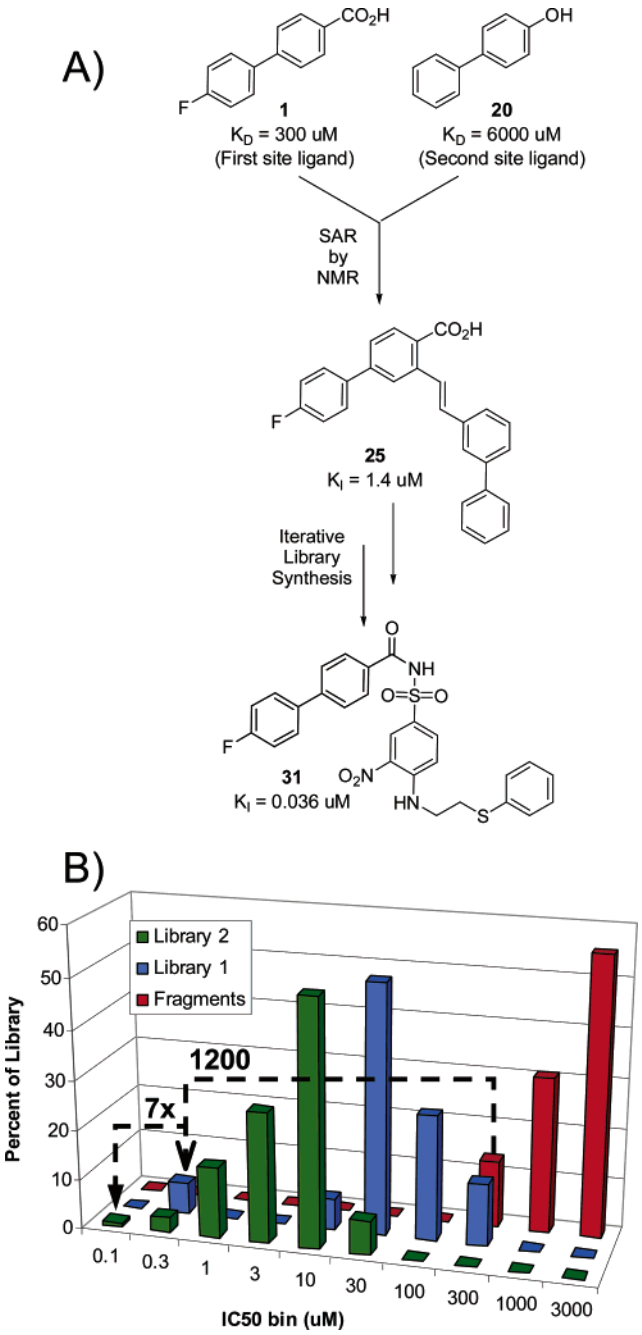

Figure 7. (A) A summary of the SAR by NMR approach as applied to Bcl-xL, in which two weakly binding ligands (**1** and **11**) that bound to proximal sites on the protein were identified and linked to produce single-digit micromolar inhibitors (**22**) of the protein. This lead was further optimized using structure-based iterative library synthesis to produce nanomolar leads (**31**). (B) A summary of the potency increases realized through the iterative library approach, in which a 1200-fold gain was obtained in the initial library and a 7-fold gain was achieved in the second iteration, resulting in a 8300-fold gain over the initial fragment leads.

available 4-chloro-3-nitrophenylsulfonyl chloride **29** was converted to the sulfonamide as described above. Acid **1** was then coupled with **29** using EDC and DMAP to yield the desired acylsulfonamide core **30**. Substitution of the chlorine in **30** with amines was easily achieved by heating the core in the presence of a 5-fold excess of the nucleophile at 100 °C in DMF overnight. A library of 125 compounds was prepared from a group of amines selected on the basis of traditional medicinal chemistry principles,[16−20] diversity calculations,[13,21,22] and molecular modeling. Of these, compound **31** (Figure 6) exhibited the highest binding affinity for Bcl-x_L, with an inhibition constant of 36 ± 2 nM.

Structural Characterization of Compound 31. To understand why **31** binds so potently to Bcl-x_L compared to other compounds in the library, an NMR-based structure of **31** bound to Bcl-x_L was determined (Figure 6). A total of 103 protein/ligand NOEs was used to dock this compound into the Bcl-x_L binding groove. The positions of the biaryl, acylsulfonamide, and nitrophenyl portions of this compound superimpose well with analogous portions of compound **28** bound to Bcl-x_L. Surprisingly, the *S*-phenyl ring is bent back underneath the nitrophenyl. This is very different from what was observed for the isothiochroman moiety of **28**. To accommodate this ligand conformation, the side chain of F97 rotates downward about $\chi 1$ and its phenyl ring is stacks against the *S*-phenyl ring of the ligand. The *S*-phenyl ring of the ligand, in turn, forms an intramolecular stack with the nitrophenyl ring, while the nitrophenyl ring stacks with Y194 of the protein. It is presumably this extensive π-stacking arrangement that accounts for the greater affinity of this ligand compared to others from the library.

Analysis of the Fragment-Based Approach. Several groups have reported on the identification of inhibitors of Bcl-x_L or Bcl-2, including antisense oligonucleotides, peptide inhibitors, and small molecule antagonists.[23] The organic small-molecule inhibitors include natural products (e.g., antimycin A and gossypol) and other compounds with liabilities that limit their therapeutic potential, such as large size, low potency, poor solubility, or synthetic intractability. In contrast, we have successfully developed a highly potent inhibitor of Bcl-x_L by independently identifying and optimizing the multiple hot spots on the protein surface and capitalizing on the combinatorial advantage of fragment-based screening (see Figure 7A). For the application to Bcl-x_L described here, the first and second-site libraries consisted of 10 000 and 3500 compounds, respectively, and the set of linkers contained 21 moieties. The product of these three libraries represents ~700 million virtual compounds—more than the total of all commercial screening libraries combined. Thus, SAR by NMR accesses significantly larger portions of chemical diversity space than do conventional lead generation methods. In addition, the structure-guided iterative library approach allowed for a highly focused and rapid optimization of the initial leads to low nanomolar potency. An 8300-fold gain in potency was realized through library optimization (see Figure 7B).

Conclusions

We have discovered a high-affinity ligand for the antiapoptotic protein Bcl-x_L through a combination of fragment-based screening (SAR by NMR) and parallel synthesis. The affinity of our initial biaryl ligand (K_d ~ 300 μM) for Bcl-x_L was increased by almost 4 orders of magnitude to obtain a lead compound with an affinity (K_i) of 36 ± 2 nM. While potent, the utility of compound **31** as a therapeutic agent was limited by its poor aqueous solubility and tight binding to serum albumin (unpublished observations). Through subsequent rounds of structure-guided synthesis these limitations were overcome and, as previously discussed,[11] a compound that causes the regression of established tumors in a mouse xenograft model was obtained. NMR-based structure determination played an important role in the discovery process, providing structural information for key intermediates and thus guiding the parallel synthesis. Finally, this study provides a fragment-based paradigm for the discovery of molecules aimed at disrupting protein−protein interactions.

Experimental Section

Protein Preparation. A previously described,[8] loop-deleted version of Bcl-x_L that lacked the putative transmembrane helix was employed in these studies. Uniformly ^{15}N-labeled protein was prepared by growing bacteria containing the Bcl-x_L plasmid on minimal media containing ^{15}N-labeled ammonium chloride as the sole nitrogen source while uniformly ^{15}N-,^{13}C-labeled protein was prepared by growing bacteria on minimal media containing ^{15}N-labeled ammonium chloride as the sole nitrogen source and ^{13}C-labeled glucose as the sole carbon source. The hexahistidine-tagged protein was purified by affinity chromatography on a nickel-ProBond column (Invitrogen), concentrated, and exchanged into 40 mM sodium phosphate buffer, pH 7.0, containing either 10% or 100% D_2O plus 5 mM deuterated dithiothreitol. Protein samples for NMR were 0.5−1.0 mM in microcells.

NMR-Based Screening. NMR-based screening was conducted by acquiring sensitivity-enhanced ^{15}N/^{1}H HSQC spectra on 500 μL of uniformly ^{15}N-labeled protein (100 μM) in the presence and absence of added compound(s). For the initial screen, 9373 compounds ($\langle$MW$\rangle \sim 210$) were added as mixtures of 10 at 1 mM each. Sixty-six of the mixtures caused significant chemical shift changes upon addition to Bcl-x_L. The first-site ligands were identified by individually testing the 660 compounds that comprised these active mixtures, yielding a total of 49 ligands exhibiting K_D values less than 5 mM. The second-site screen was performed in the presence of 2 mM 4-fluoro-biphenyl-4-carboxylic acid (**1**). In this case, 3472 compounds ($\langle$MW$\rangle \sim 150$) were added as mixtures of five at 5 mM each. The second-site ligands were identified by individually testing the 60 compounds that comprised the active mixtures, yielding a total of 24 compounds exhibiting K_d values less than 5 mM. Dissociation constants were obtained by monitoring the chemical shift changes as a function of ligand concentration using a single binding site model. A least squares grid search was performed by varying the values of K_d and the chemical shift of the fully saturated protein. Standard deviations were derived for each K_d by monitoring three different cross-peaks in the HSQC spectrum.

NMR-Based Structural Studies. NMR spectra for structural studies were recorded on Bruker DRX600 and DRX800 spectrometers at 303 K. Resonance assignments for liganded Bcl-x_L were extrapolated from those of the apo protein by comparing two-dimensional ^{13}C and ^{15}N HSQC spectra and three-dimensional ^{13}C- and ^{15}N-edited NOESY spectra of the liganded and the unliganded protein. Intraprotein NOEs for those residues of Bcl-x_L that line the binding groove were extracted from three-dimensional ^{13}C- and ^{15}N-edited NOESY spectra recorded with a mixing time of 80 ms. Protein−ligand NOEs were extracted from three-dimensional ^{13}C-edited, ^{12}C-filtered NOESY spectra recorded with mixing times ranging from 150 to 250 ms.

Structure Calculations. All structure calculations were carried out with the program CNX.[24] Initially, Bcl-x_L ligands were randomly positioned near the binding groove of the apo protein and the observed intermolecular NOEs were used to dock the ligands into the groove. This docking was followed by energy minimization and a standard simulated annealing protocol.[25] During the simulated annealing, coordinates of the protein were held fixed with the exception of those residues that line the binding groove (residues 96−112, 127−142, 191−194). This protocol was based on our structural studies of Bak peptide binding to Bcl-x_L, for which we observed structural rearrangements only for residues lining the hydrophobic groove upon peptide binding. The conformation of these residues was governed by the observed intraprotein NOEs and intermolecular NOEs.

For the initial biaryl acid, compound **1**, a total of 75 intermolecular NOEs were employed to dock the ligand to the protein. For the ternary complex of Bcl-x_L with compounds **1** and **13**, 75 intermolecular NOEs were used for compound **1** with 14 NOEs for compound **13**.

Fluorescence Polarization Assay. Assays for the inhibition of Bcl-x_L were performed in 96-well microtiter plates using a fluorescein-labeled BH3 peptide derived from the Bad protein (NLWAAQRYGRELRRMSDK(FITC)FVD) (prepared in-house) as the probe. The dissociation constant (K_d) for the binding of this peptide to Bcl-x_L is 20 nM. Test compounds were diluted in DMSO to concentrations between 100 μM and 1 pM and introduced into each well of the plate. A mixture totaling 125 μL per well of assay buffer (20 mM sodium phosphate, pH 7.4, 1 mM EDTA, 50 mM NaCl, 0.05% PF-68), 6 nM BcL-x_L protein, 1 nM fluorescein-labeled BAD peptide, and the DMSO solution of the compound was shaken for 2 min and placed in a LJL Analyst (LJL Bio Systems, CA). Polarization was measured at room temperature using a continuous fluorescein lamp (excitation 485 nm, emission 530 nm). Inhibition constants (K_i) were calculated using an in-house written program in Microsoft Excel, and the reported standard deviations are based on three measurements.

Chemistry. General Methods. All reactions were carried out under inert atmosphere (N_2) and at room temperature unless otherwise noted. Solvents and reagents were obtained commercially and were used without further purification. All reported yields are of isolated products and are not optimized. P-EDC was purchased from Polymer Laboratories and MP-TsOH was purchased from Argonaut Technologies. ^{1}H NMR spectra were obtained on a Varian UNITY or Inova (500 MHz), Varian UNITY (400 MHz), or Varian UNITY plus or Mercury (300 MHz) instrument. Chemical shifts are reported as δ values (ppm) downfield relative to TMS as an internal standard, with multiplicities reported in the usual manner. Mass spectra determinations were performed by the Analytical Research Department, Abbott Laboratories; DCI indicates chemical ionization in the presence of ammonia, ESI indicates electron spray ionization, APCI indicates atmospheric pressure chemical ionization with ammonia. Elemental analyses were performed by Quantitative Technologies, Inc., Whitehouse, NJ, or by Robertson Microlit Laboratories, Inc., Madison, NJ. Column chromatography was carried out in flash mode on silica gel (Merck Kieselgel 60, 230−400 mesh). Unless otherwise noted, preparative HPLC samples were purified on a Waters Symmetry C8 column (25 × 100 mm, 7 μm particle size) using a gradient of 10−100% CH_3CN:0.1% TFA over 8 min (10-min run time) at a flow rate of 40 mL/min. Analytical HPLC spectra were acquired on an Agilent Zorbax SB−C8 column (4.6 × 75 mm, 3.5-μm particle size) using a gradient of 30−100% CH_3CN:water over 8 min and an Agilent Zorbax SB−C18 column (4.6 × 75 mm, 3.5 μm particle size) using a gradient of 10−100% CH_3CN:water over 8 min. UV detection at 254 nm.

4′-Fluoro-3-methoxybiphenyl-4-carboxylic Acid Methyl Ester (22). A 250-mL round-bottom flask was charged with methyl 4-chloro-2-methoxybenzoate (**21**) (6.5 g, 32.5 mmol), 4-fluorophenylboronic acid (4.56 g, 32.5 mmol), and CsF (14.8 g, 97.5 mmol) followed by NMP (65 mL) and *trans*-dichlorobis(tricyclohexylphosphine)palladium(II) (0.72 g, 0.975 mmol) and was heated to 90 °C for 12 h. The resulting mixture was diluted with ethyl acetate (300 mL), washed with water and brine, dried over Na_2SO_4, and concentrated under reduced pressure. Purification by silica gel chromatography eluting with 5% ethyl acetate in hexanes yielded 6.50 g (77%) of the desired product: ^{1}H NMR (300 MHz, $CDCl_3$) δ 7.87 (d, J = 8.1 Hz, 1H), 7.59−7.53 (m, 2H), 7.18−7.10 (m, 4H), 3.97 (s, 3H), 3.91 (s, 3H); MS (DCI) m/z 261 $(M + H)^+$. Anal. ($C_{15}H_{13}FO_3$) C, H.

4′-Fluoro-3-trifluoromethanesulfonyloxybiphenyl-4-carboxylic Acid Methyl Ester (23). A solution of **22** (6.5 g, 25.0 mmol) in DCM (100 mL) was cooled to −78 °C, treated dropwise with BBr_3 (40 mL of a 1M solution in DCM, 40.0 mmol), and stirred for 2.5 h. Methanol (30 mL) was added slowly, and the mixture was allowed to warm to room temperature and concentrated under reduced pressure. Purification by silica gel chromatography eluting with 5% ethyl acetate in hexanes yielded 5.30 g (86%) of the intermediate phenol: ^{1}H NMR (400 MHz, $CDCl_3$) δ 7.87 (d, J = 8.3 Hz, 1H), 7.59−7.53 (m, 2H), 7.16−7.10 (m, 3H), 7.06 (dd, J = 8.3 Hz, J = 1.9 Hz, 1H), 3.96 (s, 3H); MS (DCI) m/z 247 $(M + H)^+$. Anal. ($C_{14}H_{11}FO_3$) C, H.

A solution of the above phenol (5.0 g, 20.7 mmol) and triethylamine (6.0 mL, 42.0 mmol) in DCM (100 mL) was cooled

to 0 °C and treated dropwise with trifluromethanesulfonic anhydride (4.53 mL, 26.9 mmol). The mixture was allowed to warm to room temperature and to stir overnight. The resulting mixture was diluted with DCM (300 mL); washed with 1.5% aqueous HCl, saturated aqueous $NaHCO_3$, water, brine; dried over Na_2SO_4; and concentrated under vacuum. Purification by silica gel chromatography eluting with 10% ethyl acetate in hexanes yielded 7.0 g (90%) of the desired product: ^{1}H NMR (400 MHz, $CDCl_3$) δ 8.15 (d, J = 8.3 Hz, 1H), 7.63 (dd, J = 8.3, 1.9 Hz, 1H), 7.59−7.53 (m, 2H), 7.44 (m, 1H), 7.21−7.16 (m, 2H), 3.99 (s, 3H); MS (DCI) m/z 396 $(M + NH_4)^+$. Anal. ($C_{15}H_{10}F_4O_3S$) C, H.

4′-Fluoro-3-vinylbiphenyl-4-carboxylic Acid Methyl Ester (24). A solution of **23** (1.51 g, 4.0 mmol) in DME (20 mL) and methanol (10 mL) was treated with vinyldibutylboronate (0.96 g, 5.2 mmol), $Pd(PPh_3)_4$ (0.23 g, 0.20 mmol), and CsF (1.82 g, 12.0 mmol). The resulting mixture was brought to reflux and stirred overnight. After allowing to cool to room temperature, the solvent was removed under vacuum and the residue partitioned between diethyl ether (300 mL) and water (60 mL). The organic layer was washed with water and brine, dried over Na_2SO_4, and concentrated under reduced pressure. Purification by silica gel chromatography eluting with 4% ethyl acetate in hexanes yielded 0.86 g (84%) of the desired product: ^{1}H NMR (400 MHz, $CDCl_3$) δ 7.96 (d, J = 8.0 Hz, 1H), 7.72 (d, J = 1.6 Hz, 1H), 7.60−7.51 (m, 3H), 7.48 (dd, J = 8.3, 1.6 Hz, 1H), 7.15 (t, J = 8.6 Hz, 2H), 5.70 (d, J = 17.2 Hz, 1H), 5.40 (d, J = 10.7 Hz, 1H), 3.92 (s, 3H); MS (DCI) m/z 257 $(M + H)^+$. Anal. ($C_{16}H_{13}FO_2$) C; H.

3-(2-Biphenyl-3-ylvinyl)-4′-fluorobiphenyl-4-carboxylic Acid (25). A solution of **24** (0.10 g, 0.40 mmol) and 3-bromobiphenyl (0.12 g, 0.50 mmol) in DMF (2 mL) and acetonitrile (4 mL) was treated with $Pd_2(dba)_3$ (0.037 g, 0.04 mmol), tri-*o*-tolylphosphine (0.025 g, 0.08 mmol), Et_3N (111 μL, 0.8 mmol) and heated to 85 °C overnight. After allowing to cool to room temperature, the mixture was concentrated under vacuum, dissolved in ethyl acetate (100 mL), washed with water and brine, dried over Na_2SO_4, and concentrated under reduced pressure. Purification by silica gel chromatography eluting with 4% ethyl acetate in hexanes yielded 0.11 g (67%) of the intermediate methyl ester: ^{1}H NMR (400 MHz, $CDCl_3$) δ 8.12 (d, J = 16.3 Hz, 1H), 8.02 (d, J = 8.3 Hz, 1H), 7.87 (d, J = 1.8 Hz, 1H), 7.75 (m, 1H), 7.64−7.61 (m, 3H), 7.58 (m, 1H), 7.52−7.42 (m, 5H), 7.38−7.34 (m, 2H), 7.17 (t, J = 8.8 Hz, 2H), 7.12 (d, J = 16.3 Hz, 1H), 3.94 (s, 3H); MS (DCI) m/z 409 $(M + H)^+$. Anal. ($C_{28}H_{21}FO_2$) C, H.

The above methyl ester (0.050 g, 0.122 mmol) was dissolved in THF (1 mL)/MeOH (0.5 mL)/H_2O (0.25 mL), treated with LiOH·H_2O (0.025 g, 0.595 mmol), and stirred overnight. The mixture was treated with 1 N HCl (2 mL) and extracted with ethyl acetate. The organic layer was washed with water and brine, dried over Na_2SO_4, and concentrated under vacuum. Purification by silica gel chromatography eluting with 3% methanol in 1:1 ethyl acetate: hexanes yielded 0.045 g (94%) of the desired product: ^{1}H NMR (400 MHz, $CDCl_3$) δ 8.09 (d, J = 6.4 Hz, 1H), 8.08 (d, J = 8.0 Hz, 1H), 7.95 (d, J = 8.3 Hz, 1H), 7.90−7.85 (m, 4H), 7.70 (d, J = 8.0 Hz, 1H), 7.67 (dd, J = 8.0, 1.6 Hz, 1H), 7.64−7.58 (m, 2H), 7.52−7.46 (m, 4H), 7.42−7.32 (m, 3H); MS (APCI) m/z 395 $(M + H)^+$, 393 $(M - H)^-$. Anal. ($C_{27}H_{19}FO_2$) C, H.

4′-Fluorobiphenyl-4-carboxylic Acid (1). To a solution of $Pd(PPh_3)_4$ (1.0 g, 0.86 mmol) in DME (250 mL) was added ethyl 4-bromobenzoate (**27**) (5.0 mL, 30.62 mmol), and the mixture was stirred at ambient temperature for 10 min. A solution of 4-fluorophenylboronic acid (5.0 g, 35.73 mmol) in EtOH (40 mL) was added and stirring was continued for 15 min. A 2 M aqueous solution of Na_2CO_3 (69 mL) was added and the reaction mixture was heated to reflux overnight. After cooling, the organic solvents were evaporated under reduced pressure, water (100 mL) and diethyl ether (200 mL) were added, and the mixture was filtered through Celite. The layers were separated, and the aqueous layer was extracted with diethyl ether. The combined organic extracts were dried over $MgSO_4$ and evaporated under reduced pressure, and the residue was purified by silica gel chromatography eluting with 33% ethyl acetate in hexanes to give 7.1 g (95%) of the intermediate ethyl ester: ^{1}H NMR (500 MHz, $CDCl_3$) δ 8.11−8.10 (m, 2H), 7.62−7.57 (m, 4H), 7.17−7.14 (m, 2H), 4.40 (q, J = 7.3 Hz, 2H), 1.42 (t, J = 7.0 Hz, 3H); MS (DCI) m/z 245 $(M + H)^+$.

A solution of the above ethyl ester (7.1 g, 29.09 mmol) in THF (80 mL)/MeOH (80 mL) was treated with a 2 N aqueous solution of NaOH (50 mL) at room temperature overnight. The reaction mixture was concentrated down to the water layer under reduced pressure and was acidified by addition of a 2 N aqueous solution of HCl. The mixture was extracted with ethyl acetate, the combined organic extracts were dried over $MgSO_4$, and the solvents were removed under reduced pressure to afford 5.94 g (94%) of the desired product: ^{1}H NMR (300 MHz, DMSO-d_6) δ 12.96 (bs, 1H), 8.04−8.01 (m, 2H), 7.82−7.76 (m, 4H), 7.37−7.29 (m, 2H); MS (DCI) m/z 216 (M^+), 234 $(M + NH_4)^+$.

Parallel Synthesis A: Acylsulfonamide Formation. The reactions were carried out in 12-mL glass vials fitted with Teflon-lined screw caps. Each vial was charged with the appropriate sulfonamide (0.31 mmol) in a mixture of $ClCH_2CH_2Cl$ (2.8 mL) and *t*-BuOH (2.8 mL). DMAP (56 mg, 0.46 mmol), **1** (100 mg, 0.46 mmol), and P-EDC (443 mg, 0.62 mmol, loading = 1.4 mmol/g) were added and the mixtures were agitated at room temperature for 24 h. Each reaction mixture was then diluted with 3 mL of ethyl acetate, MP-TsOH (561 mg, 2.3 mmol, loading = 4.1 mmol/g) was added, and agitation was continued for another 4 h. The mixtures were filtered and the solvents were evaporated under reduced pressure. The crude products were purified by preparative HPLC.

***N*-(4′-Fluorobiphenyl-4-ylcarbonyl)methanesulfonamide (26).** Compound **26** (57 mg, 63%) was obtained according to the procedure given for parallel synthesis A from **1** and methanesulfonamide: ^{1}H NMR (300 MHz, $CDCl_3$) δ 8.62 (bs, 1H), 7.93−7.90 (m, 2H), 7.70−7.67 (m, 2H), 7.62−7.57 (m, 2H), 7.21−7.15 (m, 2H), 3.47 (s, 3H); MS (DCI) m/z 311 $(M + NH_4)^+$.

***N*-(4′-Fluorobiphenyl-4-ylcarbonyl)-4-(*N*′-isothiochroman-4-ylidenehydrazino)-3-nitrobenzenesulfonamide (28).** Compound **28** (82 mg, 46%) was obtained according to the procedure given for parallel synthesis A from **1** and 4-(*N*′-isothiochroman-4-ylidenehydrazino)-3-nitrobenzenesulfonamide (Maybridge): ^{1}H NMR (400 MHz, DMSO-d_6) δ 11.04 (s, 1H), 8.73 (m, 1H), 8.18−8.16 (m, 3H), 7.98−7.95 (m, 2H), 7.81−7.77 (m, 5H), 7.37−7.28 (m, 5H), 4.03 (s, 2H), 3.88 (s, 2H); MS (ESI) m/z 577 $(M + H)^+$; HRMS (ESI) m/z calcd ($C_{28}H_{21}FN_4O_5S_2$) 577.1010, found 577.1012 $(M + H)^+$; HPLC t_R 4.627 min (C8), t_R 5.673 min (C18).

4-Chloro-3-nitrobenzenesulfonamide (29). To an ice-cooled solution of 4-chloro-3-nitrobenzenesulfonyl chloride (9.0 g, 35.0 mmol) in diethyl ether (150 mL) was added dropwise NH_4OH (66 mL, 28−30% NH_3). After the addition was complete, the ice bath was removed and the reaction mixture was stirred for an additional 30 min at room temperature. Water (100 mL) was added and the mixture was extracted with ethyl acetate. The combined organic extracts were dried over $MgSO_4$ and the solvents were removed under reduced pressure to give 8.0 g (97%) of the desired product: ^{1}H NMR (300 MHz, $CDCl_3$) δ 8.42 (d, J = 2.3 Hz, 1H), 8.05 (dd, J = 8.5, 2.0 Hz, 1H), 7.73 (d, J = 8.5 Hz, 1H), 4.94 (bs, 2H); MS (DCI) m/z 235, 237 (M^+).

4-Chloro-*N*-(4′-fluorobiphenyl-4-ylcarbonyl)-3-nitrobenzenesulfonamide (30). A mixture of **1** (5.9 g, 27.5 mmol), **29** (7.2 g, 30.3 mmol), EDC (6.3 g, 33.0 mmol), and DMAP (1.7 g, 13.8 mmol) in CH_2Cl_2 (100.0 mL) was stirred at ambient temperature for 24 h. The solvent was removed under reduced pressure and the residue was purified by silica gel chromatography eluting with 5% MeOH in DCM + 0.5% HOAc to give 6.8 g (57%) of desired product: ^{1}H NMR (300 MHz, DMSO-d_6) δ 8.63 (d, J = 2.2 Hz, 1H), 8.27 (dd, J = 8.5, 2.2 Hz, 1H), 8.07 (d, J = 8.5 Hz, 1H), 7.99−7.97 (m, 2H), 7.83−7.78 (m, 4H), 7.36−7.30 (m, 2H): MS (DCI) m/z 452 $(M + NH_4)^+$. Anal. ($C_{19}H_{12}ClFN_2O_5S$) C; H; N.

Parallel Synthesis B: Nucleophilic Substitution. The reactions were carried out in 4-mL glass vials with Teflon-lined screw caps. Each vial was charged with the appropriate amine (0.58 mmol), a stock solution of **30** (50 mg, 0.12 mmol) in DMF (2.0 mL) was added, and the mixtures were agitated and heated to 100 °C

overnight. The organic solvent was evaporated under reduced pressure and the residue was purified by preparative HPLC.

***N*-(4′-Fluorobiphenyl-4-ylcarbonyl)-3-nitro-4-(2-phenylsulfanylethylamino)benzenesulfonamide (31).** Compound **31** (14 mg, 22%) was obtained according to the procedure given for parallel synthesis B from **30** and 2-phenylthioethylamine: ^{1}H NMR (300 MHz, DMSO-d_6) δ 12.50 (bs, 1H), 8.82−8.78 (m, 1H), 8.63 (d, J = 2.0 Hz, 1H), 7.97−7.92 (m, 3H), 7.82−7.77 (m, 4H), 7.39−7.15 (m, 8H), 3.71−3.65 (m, 2H), 3.33−3.27 (m, 2H); MS m/z 552 $(M + H)^+$. Anal. ($C_{27}H_{22}FN_3O_5S_2$) C; H; N.

Supporting Information Available: Elemental analysis and HPLC data. This material is available free of charge via the Internet at http://pubs.acs.org.

References

(1) Thompson, C. B. Apoptosis in the pathogenesis and treatment of disease. *Science* **1995**, *267*, 1456−1462.
(2) Reed, J. C. Mechanisms of apoptosis. *Am. J. Pathol.* **2000**, *157*, 1415−1430.
(3) Adams, J. M.; Cory, S. The Bcl-2 protein family: Arbiters of cell survival. *Science* **1998**, *281*, 1322−1325.
(4) Cory, S.; Huang, D. C. S.; Adams, J. M. The Bcl-2 family: Roles in cell survival and oncogenesis. *Oncogene* **2003**, *22*, 8590−8607.
(5) Kitrkin, V.; Joos, S.; Zornig, M. The role of Bcl-2 family members in tumorigenesis. *Biochim. Biophys. Acta* **2004**, *1644*, 229−249.
(6) Juin, P.; Geneste, O.; Raimbaud, E.; Hickman, J. A. Shooting at survivors: Bcl-2 family members as drug targets for cancer. *Biochim. Biophys. Acta* **2004**, *1644*, 251−260.
(7) Petros, A. M.; Olejniczak, E. T.; Fesik, S. W. Structural biology of the Bcl-2 family of proteins. *Biochim. Biophys. Acta* **2004**, *1644*, 83−94.
(8) Sattler, M.; Liang, H.; Nettesheim, D.; Meadows, R. P.; Harlan, J. E.; et al. Structure of Bcl-xL−Bak peptide complex: Recognition between regulators of apoptosis. *Science* **1997**, *275*, 983−986.
(9) Petros, A. M.; Nettesheim, D. G.; Wang, Y.; Olejniczak, E. T.; Meadows, R. P.; et al. Rationale for Bcl-xL/Bad peptide complex formation from structure, mutagenesis, and biophysical studies. *Protein Sci.* **2000**, *9*, 2528−2534.
(10) Arkin, M. R.; Wells, J. A. Small-molecule inhibitors of protein−protein interactions: Progressing towards the dream. *Nat. Rev. Drug Discovery* **2004**, *3*, 301−317.
(11) Oltersdorf, T.; Elmore, S. W.; Shoemaker, A. R.; Armstrong, R. C.; Augeri, D. J.; et al. An inhibitor of Bcl-2 family proteins induces regression of solid tumors. *Nature* **2005**, *435*, 677−681.
(12) Zhang, H.; Nimmer, P.; Rosenberg, S. H.; Ng, S. C.; Joseph, M. Development of a high-throughput fluorescence polarization assay for Bcl-xL. *Anal. Biochem.* **2002**, *307*, 70−75.
(13) Martin, Y. C. Molecular diversity: How we measure it? Has it lived up to its promise? *Farmaco* **2001**, *56*, 137−139.
(14) Sturino, F. S.; Labelle, M. A convenient method for the preparation of acylsulfonamide libraries. *Tetrahedron Lett.* **1998**, *39*, 5891−5894.
(15) Lobb, K. L.; Hipskind, P. A.; Aikins, J. A.; Alvarez, E.; Cheung, Y. Y.; et al. Acyl sulfonamide anti-proliferatives: Benzene substituent structure−activity relationships for a novel class of antitumor agents. *J. Med. Chem.* **2004**, *47*, 5367−5380.
(16) Hansch, C.; Unger, S. H.; Forsythe, A. Strategy in drug design. Cluster analysis as an aid in the selection of substituents. *J. Med. Chem.* **1973**, *16*, 1217−1222.
(17) Topliss, J. G. A manual method for applying the Hansch approach to drug design. *J. Med. Chem.* **1977**, *20*, 463−469.
(18) Craig, P. N. *The Basis of Medicinal Chemistry*; Wiley-Interscience: New York, 1980.
(19) Wermuth, C. G. *Agressologie* **1966**, *7*, 213.
(20) Lipinski, C. Tools for oral absorption, part two. Predicting human absorption. *BIOTEC, PDD symposium*, AAPS: Miami, FL, 1995.
(21) Brown, R. D.; Martin, Y. C. An evaluation of structural descriptors and clustering methods for use in diversity selection. *QSAR Environ. Res.* **1998**, *8*, 23−29.
(22) Barnard, J. M.; Downs, G. M. Clustering of chemical structures on the basis of two-dimensional similarity measures. *Inf. Comput. Sci.* **1992**, *32*, 644−649.
(23) Pulley, H.; Mohammad, R. Small-molecule inhibitors of Bcl-2 protein. *Drugs Future* **2004**, *29*, 369−381.
(24) Brunger, A. T. *X-PLOR Version 3.1*; Yale University Press: New Haven, 1992.
(25) Kuszewski, J.; Nigles, M.; Brunger, A. T. *J. Biomol. NMR* **1992**, *2*, 33−38.

JM0507532